

## Dynamical Hall Effect in a Two-Dimensional Classical Plasma

D. C. Glatli, E. Y. Andrei, G. Deville, J. Poitrenaud, and F. I. B. Williams

*Service de Physique du Solide et de Résonance Magnétique, Centre d'Etudes Nucléaires de Saclay,  
F-91191 Gif-sur-Yvette Cedex, France*

(Received 16 January 1985)

We have shown that the collective modes of a bounded two-dimensional plasma in a magnetic field exhibit unexpected features which are dynamical manifestations of the Hall effect. In high fields we observed the appearance of a novel magnetically localized one-dimensional wave which propagates along the perimeter of the plasma.

PACS numbers: 73.20.Cw, 71.45.Gm, 72.15.Gd

The Lorentz force acting on a bounded system of charge carriers in a magnetic field can induce charge accumulation at the boundaries. The Hall resistance, which is a stationary manifestation of this phenomenon, has traditionally been exploited to measure the charge carrier density. But it has not yet been recognized that the dynamics of a plasma in a magnetic field in the presence of density inhomogeneity (in particular boundaries) has physical aspects which are more general than the Hall resistance. In this Letter we present the first theoretical and experimental results on the dynamical Hall effect in a two-dimensional classical plasma. The theoretical results obtained in a linearized frictionless hydrodynamic approach will be compared with measurements of the plasmon mode frequencies of electrons confined on a liquid helium surface in a cylindrical cell placed in a normal magnetic field  $H\hat{z}$ . The spectrum and its behavior with magnetic field can be seen in Figs. 1 and 2. An unusual feature is the existence of modes whose frequencies decrease with field, in contradiction to the generally used infinite-geometry rule  $\omega^2 = \omega_p^2(H=0) + \omega_c^2$  where  $\omega_p(H=0)$  is the zero-field plasmon frequency and  $\omega_c = eH/mc$  is the cyclotron frequency.<sup>1</sup> We shall show that this decrease is one of the dynamical manifestations of the Hall effect.

We suppose the electrons of mass  $m$  and charge  $e$  to be confined to a single region of the plane  $z=0$  by a set of externally imposed potentials which determine the equilibrium charge distribution  $n_s(\mathbf{r}) = n_0\sigma(\mathbf{r})$  where  $\mathbf{r}$  is a two-dimensional position vector. We will now show that the hydrodynamic problem can be reduced to an electrostatic one. The only force relevant to their dynamics arises from the in-plane component of the (total) electrostatic field described by a scalar potential  $\phi(\mathbf{r}, z, t)$ . The equation of motion of the electron beam is thus  $d\mathbf{v}/dt = (e/m)\nabla\phi + \omega_c \times \mathbf{v}$  where  $\mathbf{v}$  is the velocity field and  $\omega_c = \omega_c\hat{z}$ . If we suppose a time variation  $\phi = \phi(\mathbf{r}, z)\exp i\omega t$ , we can combine the linearized equation of motion rewritten as

$$\mathbf{v} = (e/m)(\nabla_2\dot{\phi} + \omega_c \times \nabla_2\phi)/(\omega_c^2 - \omega^2) \quad (1)$$

with the linearized continuity equation and a Gauss integral of Poisson's equation to write the boundary con-

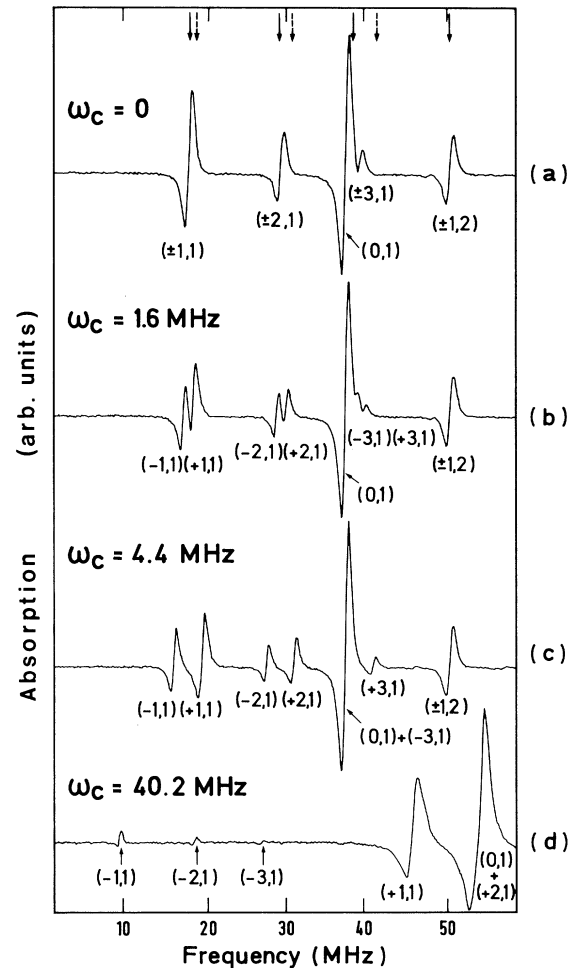


FIG. 1. Part of the longitudinal spectrum of electrons of density  $n_0 = 1.7 \times 10^7 \text{ cm}^{-2}$  obtained at  $T = 60 \text{ mK}$ . The upper-plate, guard-ring, and corresponding electron-surface potentials are respectively  $-3$ ,  $-7$ , and  $-3 \text{ V}$ . The solid and dashed arrows of (a) indicate the calculated mode frequencies with and without the density profile correction. For this density the solid-phase vibration frequency of the electron in the individual dimple it creates at the surface is  $\omega_0 \leq 1 \text{ MHz}$  and can be neglected. The applied magnetic field is denoted by the free-electron cyclotron frequency  $\omega_c$ . The (4,1) mode is weak and hidden in the wing of the (1,2) mode.

dition for the potential at the charges:

$$\frac{q}{2} \left( \frac{\partial \phi}{\partial z} \Big|_{z=0^-} - \frac{\partial \phi}{\partial z} \Big|_{z=0^+} \right) + \nabla_2 \cdot (\sigma \nabla_2 \phi) + \frac{i\omega_c}{\omega} \cdot (\nabla_2 \sigma \times \nabla_2 \phi) = 0 \quad (2)$$

where  $\omega^2 - \omega_c^2 = 2\pi n_0 e^2 q/m$  and  $\nabla_2 = \hat{x}\partial/\partial x + \hat{y}\partial/\partial y$ ,  $\nabla^2 \phi = 0$  everywhere else and  $\phi = 0$  on the metallic confining electrodes.

We see from (1) that the local current  $\mathbf{j} = -en_s(\mathbf{r})\mathbf{v}$  is the sum of a longitudinal current  $\mathbf{j}_l = \gamma_l(\mathbf{r}, \omega)\mathbf{E}$ , due to the (total) electric field  $\mathbf{E} = -\nabla_2 \phi$  induced by charge motion, and a transverse current  $\mathbf{j}_t = \gamma_t(\mathbf{r}, \omega)\hat{z} \times \mathbf{E}$ , due to the Lorentz force, where  $\gamma_t = (1 - \omega^2/\omega_c^2)^{-1} cen_s(\mathbf{r})/H$  and  $\gamma_l = \gamma_t i\omega/\omega_c$  are the nondiagonal and diagonal parts of a local ac conductivity tensor  $\gamma$ . The last term in (2) originates from the continuity equation  $\partial n/\partial t + \nabla \cdot \mathbf{j}_t = \mathbf{j}_l \cdot \nabla \sigma/\sigma$ , where  $n(\mathbf{r}, t)$  is the induced density, which shows that inhomogeneity, necessarily present for a finite-size sample, couples the transverse current to the compression, except in the case of  $\mathbf{j}_t \perp \nabla \sigma$ . This is the dynamical Hall effect. We study it in the experimental configuration of electrons condensed onto the liquid helium surface ( $z = 0$ ) of a half-filled cylindrical cell of height  $D = 2$  mm and confined laterally by a circular guard ring<sup>2</sup> of radius  $R = 9$  mm. The electrons form a disk whose radius  $R_0$ , charge distribution  $n_s(\mathbf{r})$ , and potential ( $-U$ ) are

uniquely determined by the static confined potentials:  $-W$  on the guard ring, 0 on the lower electrode,  $-V$  on the upper electrode. The independent potentials allow us to reduce the pressing field at low temperatures without losing the electrons. The disk radius  $R_0 = R - s$  is obtained through  $\sinh^2(\pi s/2D) = (W - U)/(2U - V)$ . The characteristic length of the edge inhomogeneity of the static density profile  $n_s = n_0 \sigma(\mathbf{r})$  is  $D/\pi \ll R$ . The density presents a limiting behavior  $(R - s - r)^{1/2}$  at the edge and a plateau  $n_s(r \leq R - s - D/\pi) = n_0 = (2U - V)/2\pi eD$  near the center.<sup>3</sup> In this particular static configuration, the solutions for the eigenmodes take the form of clockwise and anticlockwise rotating waves  $\phi_{\pm\nu, \mu}(r, z) \times \cos[\omega(k_{\pm\nu, \mu})t \pm \nu\theta]$  and radial waves (when the integer  $\nu$  is zero), whose dispersion relation is

$$\omega^2(k) = \omega_c^2 + (2\pi n_0 e^2/m)k \tanh(kD/2). \quad (3)$$

The wave numbers  $k_{\nu, \mu}$ , to order  $(D/\pi R)^2$  and when  $k_{\nu, \mu} D \leq 1$ , are given by<sup>3,4</sup>

$$k_{\pm\nu, \mu} R^* J'_\nu(k_{\pm\nu, \mu} R^*) = \left[ -\nu^2 \frac{D}{\pi R^*} \cosh \psi \ln \left[ \tanh \frac{\psi}{2} \right] \mp \nu \frac{\omega_c}{\omega_{\pm\nu, \mu}} \left[ 1 - \frac{D}{\pi R^*} \ln \frac{2}{\tanh \psi} \right] \right] J_\nu(k_{\pm\nu, \mu} R^*), \quad (4)$$

where  $\psi = \pi s/D$  and

$$R^* = \int_0^{R-s} dr/\sigma(r) \simeq R - s - (D/\pi) \ln[\tanh \psi (1 - e^{-4\psi})/4]$$

is an effective radius (or "optical path") for the plasmon wave.  $J_\nu$  and  $J'_\nu$  are the integer Bessel function and its derivative, and  $\omega_{\pm\nu, \mu} = \omega(k_{\pm\nu, \mu})$ . The dispersion relation (3) is the same as for an infinite medium,<sup>1</sup> but the wave numbers  $k_{\pm\nu, \mu}$  are a function of the magnetic field through  $\omega_c$  and of the precise density profile through  $\psi(U, V, W)$ . The manifestations of the dynamical Hall effect are contained in Eq. (4). For  $h = 0$  each azimuthal mode  $(\pm\nu, \mu)$  is doubly degenerate:  $k_{\nu, \mu} = k_{-\nu, \mu}$ . In a magnetic field the wave numbers  $k_{0, \mu}$  of the radial modes are unchanged, since the transverse current has no component in the radial direction. However, the double degeneracy of the azimuthal modes is lifted through the breaking of the reflection symmetry by the Lorentz force and the mode frequencies split linearly in weak field ( $\omega_c \ll \omega_{\pm\nu, \mu}$ ).

It is simpler (and no physics is lost) to discuss the solution of (4) in the limit  $D/\pi R^* \rightarrow 0$ . In this case the density is a step function [ $\sigma(r) = 1, r \leq R - s$ , and

zero otherwise],  $R^* = R - s$ ,

$$\phi_{\pm\nu, \mu}(z = 0) = J_\nu(k_{\pm\nu, \mu} r) \cos(\omega t \pm \nu\theta)$$

for  $r \leq R - s$ , and Eq. (4) is equivalent to the vanishing of the radial velocity on the disk edge. In high field, the mode frequencies all tend asymptotically towards the line  $\omega = \omega_c$ , except for the slowest modes  $(-\nu, 1)$  which cross the line  $\omega = \omega_c$  when  $\omega_c = c_p[\nu(\nu + 1)]^{1/2}/R_0$ , where  $c_p = (\pi n_0 e^2 D/m)^{1/2}$  is the screened plasmon velocity. On further increase of  $\omega_c$ , the solutions for  $k_{-\nu, 1}$  become imaginary,  $k_{-\nu, 1} = iK_{-\nu}$ , and  $\omega_{\nu, 1}^2 = \omega_c^2 - c_p^2 K_{-\nu}^2$ . As  $J_\nu(ix) = I_\nu(x) \sim e^x/(2\pi x)^{1/2}$  for  $x \gg 1$ , the wave becomes localized near the edge within a strip of width  $c_p/\omega_c$  so tending to a one-dimensional mode of frequency  $\omega_{-\nu, 1} = \nu c_p/R_0$  which propagates with a velocity  $c_p$ . This perimeter wave is analogous to the Rayleigh surface wave in a solid where the transverse force is replaced by the Lorentz force.<sup>5</sup> We note that in this limit

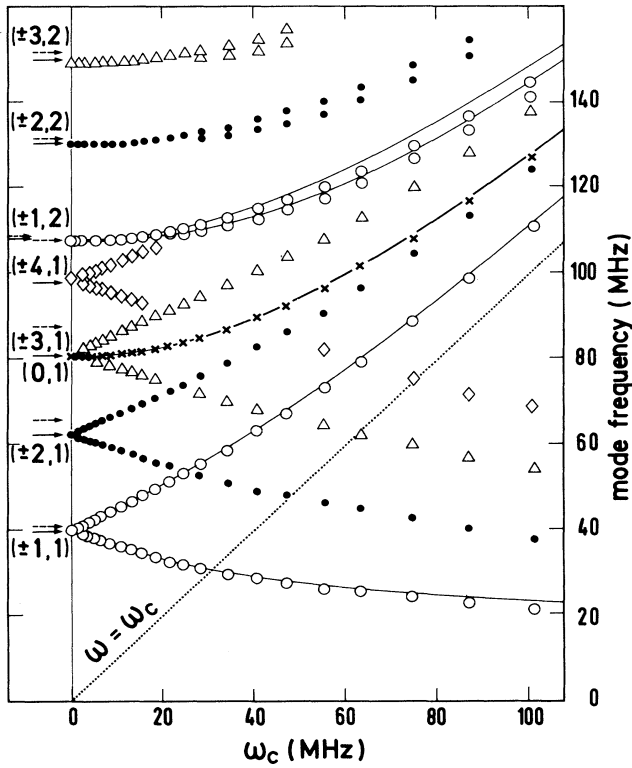


FIG. 2. The longitudinal mode frequencies vs magnetic field for a density  $n_0 = 7.2 \times 10^7 \text{ cm}^{-2}$  at  $T = 60 \text{ mK}$ . For clarity the comparison with the frequencies calculated from Eq. (4) (solid lines) is limited to the modes (0,1),  $(\pm 1, 1)$ ,  $(\pm 1, 2)$ . The upper-electrode, guard-ring, and corresponding electron surface potentials are respectively  $-6$ ,  $-40$ , and  $-9 \text{ V}$ . The solid and dashed arrows indicate the zero-field calculated frequencies with and without the density-profile correction. All the calculated frequencies (arrows and solid line) take into account the small effect of  $\omega_0$  which is estimated to be  $10 \pm 2 \text{ MHz}$  [according to extensive measurements made previously (Refs. 2 and 7)]. The line  $\omega = \omega_c$  is drawn as a guide (i.e.,  $\omega_c = 2.8 \text{ MHz/G}$  or  $100 \text{ MHz}$  corresponds to  $H = 37.7 \text{ G}$ ). There are no adjustable parameters.

$v_r \approx 0$  everywhere and the current  $I(\omega t + \nu\theta) = \int_0^{R-s} j_\theta n_s dr$ , in phase with the potential  $\phi(r, \omega t + \nu\theta)$ , satisfies  $IR_H = \phi|_{r=R} - \phi|_{r=0}$  where  $R_H = H/(cen_0)$  is the static Hall resistance.

These results are consistent with our measurements. The modes are excited by a meander transmission line on the lower electrode carrying about  $1 \text{ nW}$  of radio-frequency power from a swept  $1\text{--}400\text{-MHz}$  source to a detector. The line couples to the electrons by a potential described by  $\phi_L(\mathbf{r}, t) = \phi_L \exp(i(\omega t - \mathbf{k}_L \cdot \mathbf{r} \cos\theta))$ , where  $\mathbf{k}_L = \hat{\mathbf{x}}\omega/v_L$  is directed along the symmetry axis of the line,  $\hat{\mathbf{x}} \cdot \hat{\mathbf{r}} = \cos\theta$ , and  $v_L = 10^8 \text{ cm/sec}$  is the phase velocity of the principal mode of the line.<sup>2</sup> Rewriting  $\phi_L(\mathbf{r}, t)$  as  $\phi_L \sum_{\nu=-\infty}^{+\infty} (i)^\nu J_\nu(k_L r) \exp(i(\omega t$

$-\nu\theta)$  shows that both radial ( $\nu=0$ ) and azimuthal ( $\nu \neq 0$ ) modes are excited and the coupling is a calculable decreasing function of  $|k_L - k_{\pm\nu, \mu}|$ . A low-frequency phase-sensitive detector synchronized with the modulated upper electrode furnishes an output signal which is the derivative of the absorption spectrum with respect to the pressing field. Part of the experimental spectrum at charge density  $n_0 = 1.7 \times 10^7 \text{ cm}^{-2}$  at  $T = 60 \text{ mK}$  is shown in Fig. 1. Figure 1(a) corresponds to zero magnetic field. The absorption modes  $(\pm\nu, \mu)$  are unambiguously identified.<sup>6</sup> The solid arrows and the dashed arrows indicate the frequencies calculated from either Eq. (4) or its limit  $D/\pi R^* \rightarrow 0$  for  $H=0$ . This shows that the edge inhomogeneity modifies quantitatively the azimuthal modes. The radial mode frequency is used as a reference from which the charge density is deduced. When a small magnetic field is applied, the azimuthal modes exhibit the splittings shown in Figs. 1(b) and 1(c). Figure 2 displays the magnetic field dependence of the lowest fifteen modes for a sample of density  $n_0 = 7.2 \times 10^7 \text{ cm}^{-2}$  and the experimental data are compared to the calculated values for the modes (0,1),  $(\pm 1, 1)$ ,  $(\pm 1, 2)$  (solid lines). In higher field we distinguish between two types of modes: (i) the modes whose frequency is higher than  $\omega_c$  and combines nearly quadratically with  $\omega_c$  as expected for cycloplasmons in an infinite geometry; (ii) the modes  $(-\nu, 1)$  whose frequency drops below  $\omega_c$ , a novel feature which is the signature of a wave that propagates on the plasma perimeter. The amplitude of these modes decreases with decreasing field which indicates that fewer and fewer electrons participate in the motion as the wave becomes localized at the sample edge within a strip of width  $\sim 1/H$ . The asymptotic frequencies are expected to be  $\nu c_p/R^*$  in the idealized case (step density profile and screened interaction), but the experimental agreement is less good ( $c_p/R^* = 21.6 \text{ MHz}$  for  $n_0 = 7.2 \times 10^7 \text{ cm}^{-2}$ ). In this picture, the wave is localized in a strip  $c_p/\omega_c$  which is of the same order as the characteristic decay length of the density and the dynamical screening length  $D/\pi$ . In this case, formula (4) is no longer valid and we can expect a behavior of the frequency in high magnetic field similar to the unscreened case (i.e.,  $\omega \sim 1/\omega_c$ , see Ref. 4).

Correlational effects seem to be unimportant: For all the samples studied, we were able to work at temperatures above and below the melting of the electron solid at  $T = T_m$ . When the temperature was swept through  $T_m$ , we observed the appearance of the electron-ripplon coupled modes<sup>7,8</sup> but the feature related to Hall charge accumulation remained. To incorporate the transverse excitations  $\omega_t = (c_t^2 k^2 + \omega_0^2)^{1/2}$  into our results, where  $c_t$  denotes the transverse velocity, we must divide the factor  $\nu\omega_c/\omega$  in Eq. (4) (in the limit  $D/\pi R \rightarrow 0$ ) by  $1 - \omega_t^2/\omega^2$  and the new dispersion

relation becomes  $(\omega^2 - \omega_0^2 - c_p^2 k^2)(\omega^2 - \omega_l^2) = \omega^2 \omega_c^2$ , where  $\omega_0$  denotes the local mode frequency in the electron dimple.<sup>7,8</sup>

The new features of the spectrum in a magnetic field are not peculiar to the circular geometry and in particular the new one-dimensional perimeter wave is expected to exist in other two-dimensional systems and might well be used as a local probe. For example, it could be put to use to study the decay of correlations in the crystalline phase due to the diminishing density towards the edge of the sample. We speculate that the dynamical Hall effect can also be employed to study the quantized Hall effect: We expect that plasmon waves can propagate when the Fermi level lies in the extended states region. The plasmon-wave frequency  $\omega_p(k)$  is  $\sim (n_f)^{1/2}$  where  $n_f$  is the density of delocalized states [with  $\omega_p \ll \omega_c$  and  $k \ll (eH/c\hbar)^{1/2}$ ]. With a suitable metallic screening, a wave in high magnetic field could be localized near the edge of the sample in a strip  $\leq 1 \mu\text{m}$  and might give information about the spatial distribution of the extended states.

During the course of this work, another group<sup>9</sup> reported the observation of new, as then unexplained, magnetoplasmon modes in a rectangular geometry at high density. We think that the dynamical Hall effect is also responsible for these modes but the appearance of a large local mode frequency in the solid phase and the rectangular geometry make the analysis more difficult.<sup>10</sup>

We would like to thank D. Marty, V. Shikin, D. Estève, and M. Devoret for helpful discussions and critical reading of the manuscript and C. Heyer-Ricoul for technical assistance.

<sup>1</sup>A. V. Chaplik, Zh. Eksp. Teor. Fiz. **62**, 746 (1972) [Sov. Phys. JETP **35**, 395 (1972)].

<sup>2</sup>G. Deville, A. Valdes, E. Y. Andrei, and F. I. B. Williams,

Phys. Rev. Lett. **53**, 588 (1984). In the present experiment the excitation of the line at  $k = 520 \text{ cm}^{-1}$  does not contribute because the electron surface is too far ( $\sim 1 \text{ mm}$ ) from the line.

<sup>3</sup>D. C. Glatli *et al.*, to be published. A precise form of the density profile is found by conformal mapping in the case  $R \gg D$ . For  $r \leq R - s$ , we found

$$\sigma(r) = \frac{\{\sinh[(R-r-s)\pi/D] \sinh[(R-r+s)\pi/D]\}^{1/2}}{\cosh[(R-r)\pi/D]}.$$

<sup>4</sup>The formula (4) is not valid when  $|(\omega_c - \omega)/\omega_c| \ll D/\pi R$ . In this regime we can use an expansion around an exact solution at  $\omega_{-\nu,1} = \omega_c$ . In addition in the case  $\nu/R \gg 1/D$  (and then  $k_{\pm\nu,\mu} D \gg 1$ ) when the interactions are not screened, we found an exact solution using parabolic cylinder coordinates which gives the dispersion relation for the  $(\pm\nu, 1)$  modes:

$$\omega^2 \pm \omega \omega_c - \frac{\pi}{2} \left( \tanh \frac{\pi s}{D} \right) \left( \frac{R-s}{\nu D} \right)^{1/2} \omega_p^2 \left( \frac{\nu}{R-s} \right) = 0.$$

<sup>5</sup>L. D. Landau and E. M. Lifshitz, *Theory of Elasticity* (Pergamon, Oxford, 1959); B. A. Auld, *Acoustic Fields and Waves in Solids* (Wiley, New York, 1973), Vol. 2. In three dimensions magnetoplasmon surface waves are also found: K. W. Chiu and J. J. Quinn, Phys. Rev. B **5**, 4707 (1972).

<sup>6</sup>The narrow linewidths necessary to detect the splittings require low holding field (low density and temperature). The localization of the perimeter mode by the magnetic field results in reduced absorption amplitude and, for solenoidal field excitation, the lower frequency means smaller coupling. In particular, these modes lie outside the field-frequency window of the experiments described in Refs. 2 and 7.

<sup>7</sup>F. Gallet, G. Deville, A. Valdes, and F. I. B. Williams, Phys. Rev. Lett. **49**, 212 (1982).

<sup>8</sup>C. C. Grimes and G. Adams, Phys. Rev. Lett. **42**, 795 (1979); D. Fisher, B. I. Halperin, and P. M. Platzman, Phys. Rev. Lett. **42**, 798 (1979).

<sup>9</sup>D. B. Mast and A. J. Dahm, Physica (Utrecht) **126B**, 457 (1985).

<sup>10</sup>After submittal of the present work, we received a paper from D. B. Mast, A. J. Dahm, and A. L. Fetter [Phys. Rev. Lett. **54**, 1706 (1983)] in which an explanation is proposed for some of the modes of Ref. 9 as edge waves in an unscreened approximation.